Supporting Information containing 17 pages, 12 figures and 3 tables to accompany manuscript titled

A Modified Double Potential Step Chronoamperometry (DPSC) Method for As(III) Electro-oxidation and Concomitant As(V) Adsorption from Groundwaters

Zhao Song,[a] Shikha Garg,[a] Jinxing Ma[a] and T. David Waite[a,*]

[a] *UNSW Water Research Centre, School of Civil and Environmental Engineering, The University of New South Wales, Sydney, NSW 2052, Australia*

S1: Additional experimental details

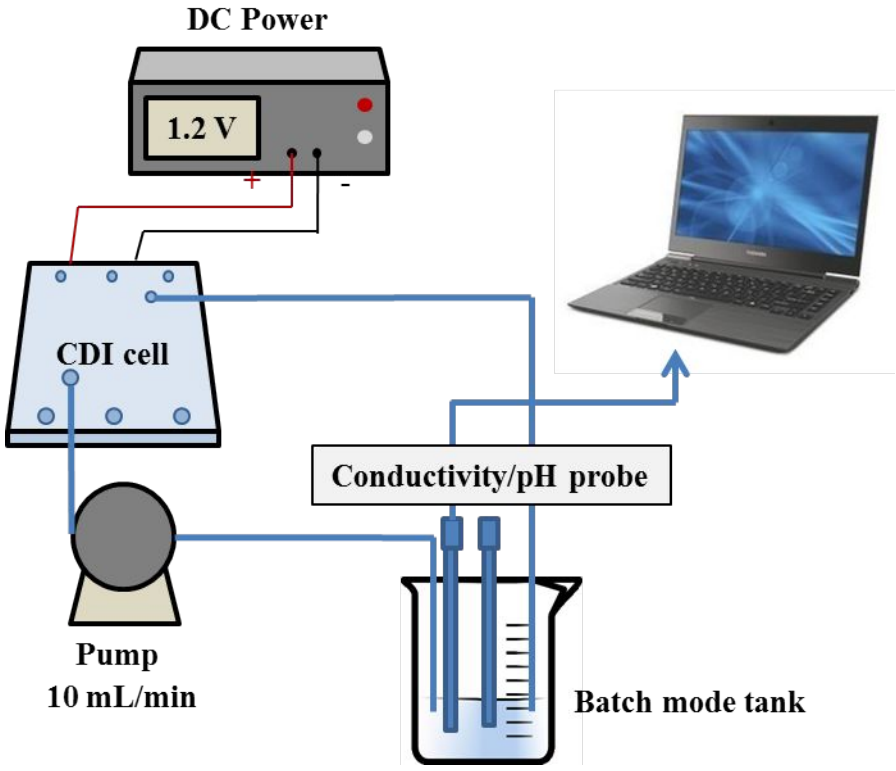

Figure S1. DPSC experimental setup

S1.1 Calculation of electrode potential of the Ag/AgCl reference electrode

The electrode potential of Ag/AgCl at a given NaCl concentration was calculated using eq. S1. Furthermore, a correction factor of -0.07 V was applied to account for the difference in standard electrode potential of commercial Ag/AgCl electrode and the self-made Ag/AgCl electrode used here.

$$E = E_0 + 0.059 \log \frac{K_{sp}}{[Cl^-]} \quad \text{(S1)}$$

When 5 mM NaCl is used as electrolyte

$$E = -0.07 + 0.799 + 0.059 \log \frac{1.8 \times 10^{-10}}{5 \times 10^{-3}} = 0.29V \quad \text{(S2)}$$

Table S1. LC isocratic method and ICP-MS operating parameters.

Parameter	Setting
Mobile Phase	10 mM Ammonium Nitrate and 10 mM Ammonium Phosphate (dibasic)
Flow Rate	0.6 mL/min
Column	Anion Exchange, Hamilton PRP-X100, 4.1 mm i.d. × 250 mm, 10 µm
Column Temperature	Ambient
pH	6.2
Autosampler Flush Solvent	5% Methanol/95% DI Type I Water
Sample Injection Volume	100 µL
Total Analysis Time	8 min
RF Power	1500 w
Plasma Ar Flow	15 L/min
Nebulizer Ar Flow	1 L/min
Aux. Ar Flow	1 L/min
Monitored Ion m/z	75 (75As)
He gas Flow	0.35 mL/min

S2: Additional experimental results

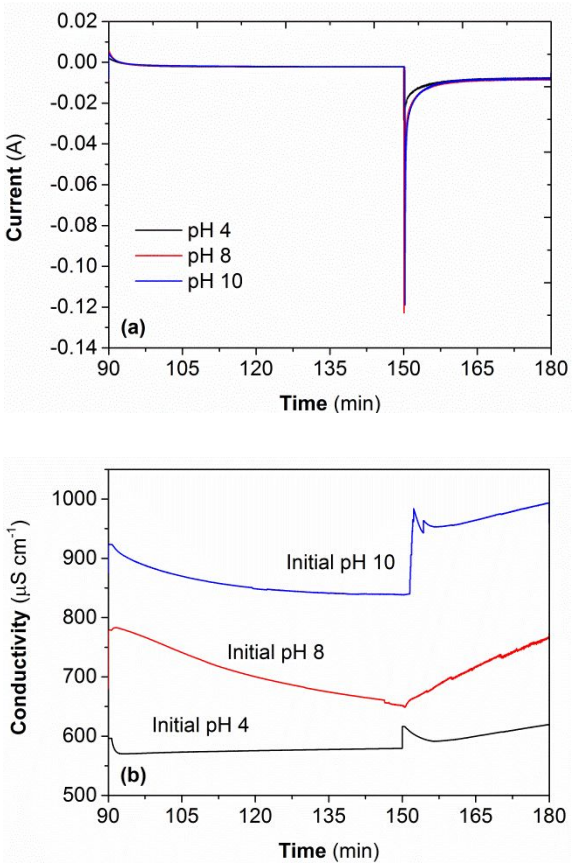

Figure S2. Changes in (a) current and (b) conductivity when the modified DPSC commenced with initial pH 4, 8 and 10. Experimental conditions: the feed solution contained C_0 = 150 μg L^{-1} As(V) and 5 mM NaCl. The initial pHs of 4, 8 and 10 were respectively controlled by addition of HCl (<0.1 mM), 2 mM $NaHCO_3$, and 1 mM $NaHCO_3$ and 1 mM Na_2CO_3. 1.2 V was applied at the first step for 60 min followed by −1.2 V for 30 min.

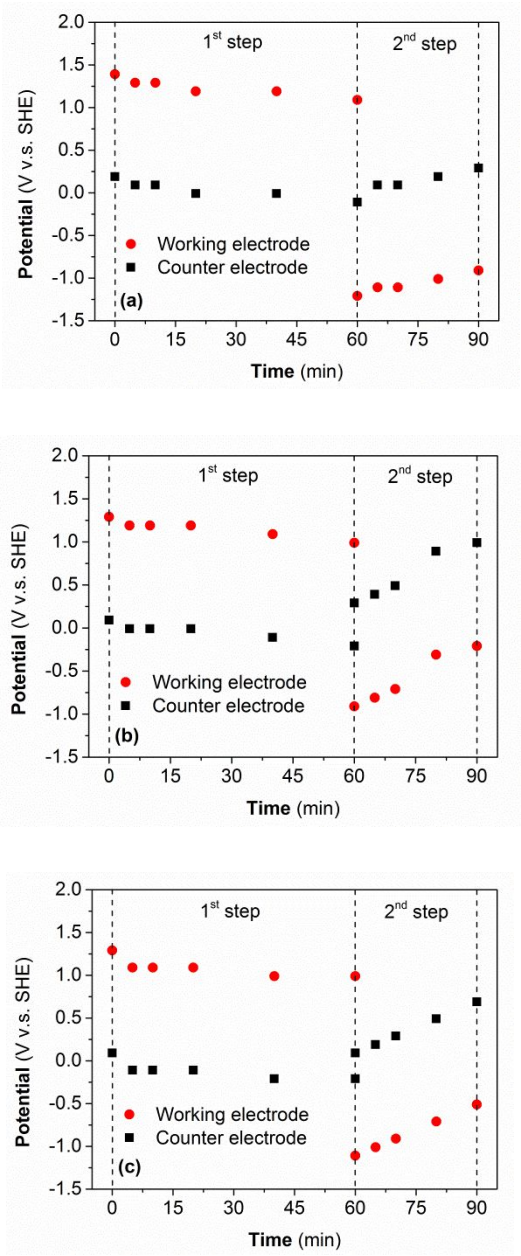

Figure S3. Changes in the potentials of working electrode and counter electrode versus standard hydrogen electrode (SHE) during As(III) removal at initial pH (a) 4, (b) 8 and (c) 10 during the first step and second step. Experimental conditions: the feed solution contained C_0 = 150 μg L^{-1} As(V) and 5 mM NaCl. The initial pHs of 4, 8 and 10 were respectively controlled by addition of HCl (<0.1 mM), 2 mM $NaHCO_3$, and 1 mM $NaHCO_3$ and 1 mM Na_2CO_3. 1.2 V was applied at the first step for 60 min followed by −1.2 V for 30 min.

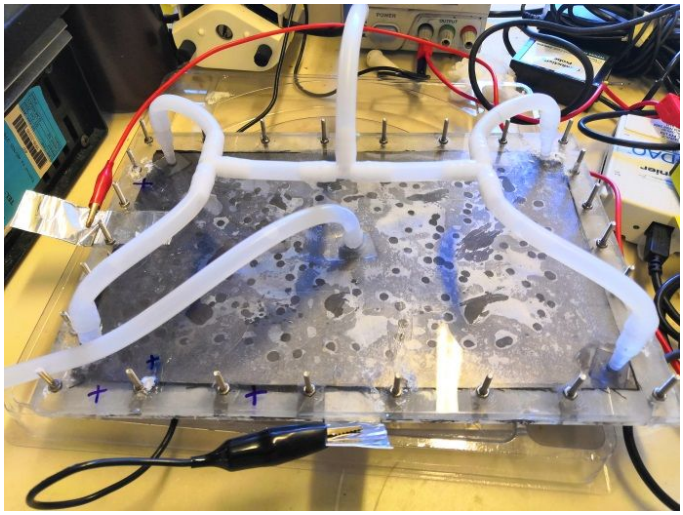

Figure S4. The 3rd electrochemical cell with the electrode area of 27 cm × 17 cm.

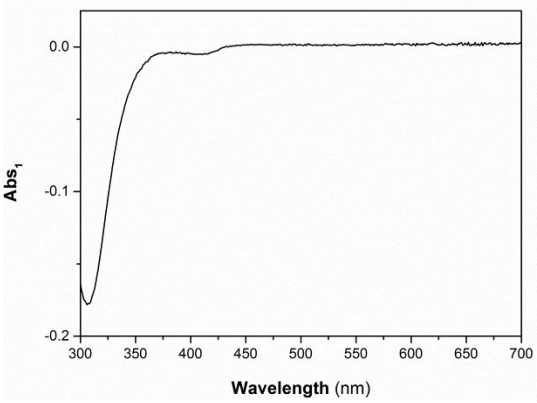

Figure S5. Measured absorbance A_1 corresponding to OCl^- formation in the experimental solution when the modified DPSC commenced with initial pH 8 at 1.2 V after 60-min adsorption. Experimental conditions: the feed solution contained C_0 = 150 µg L^{-1} As(III) and 5 mM NaCl.

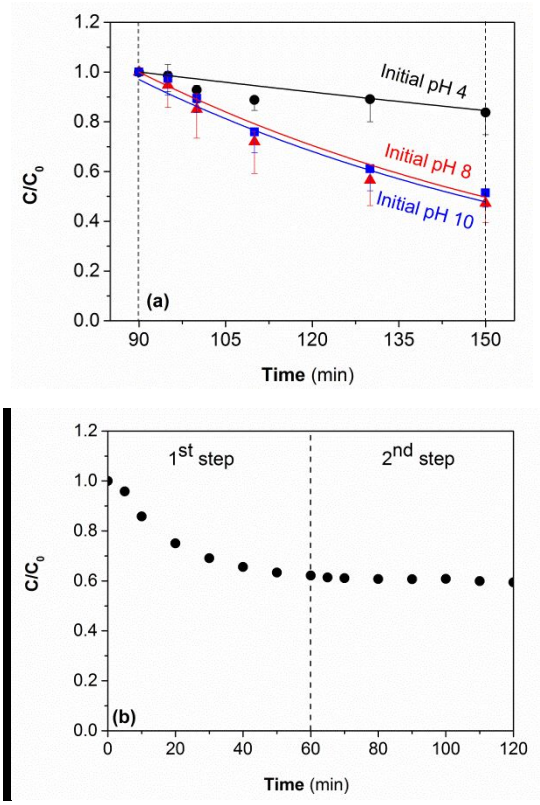

Figure S6. (a) Changes in aqueous As(V) concentrations when the modified DPSC commenced with initial pHs of 4, 8 and 10. Experimental conditions: the feed solution contained C_0 = 150 μg L^{-1} As(V) and 5 mM NaCl. The initial pHs of 4, 8 and 10 were respectively controlled by addition of HCl (<0.1 mM), 2 mM $NaHCO_3$, and 1 mM $NaHCO_3$ and 1 mM Na_2CO_3. No voltage was applied. (b) Changes in aqueous As(V) concentrations when the modified DPSC commenced with initial pH 4. Experimental conditions: the feed solution contained C_0 = 150 μg L^{-1} As(V) and 5 mM NaCl. 1.2 V was applied at the first step for 60 min followed by 0 V for 30 min.

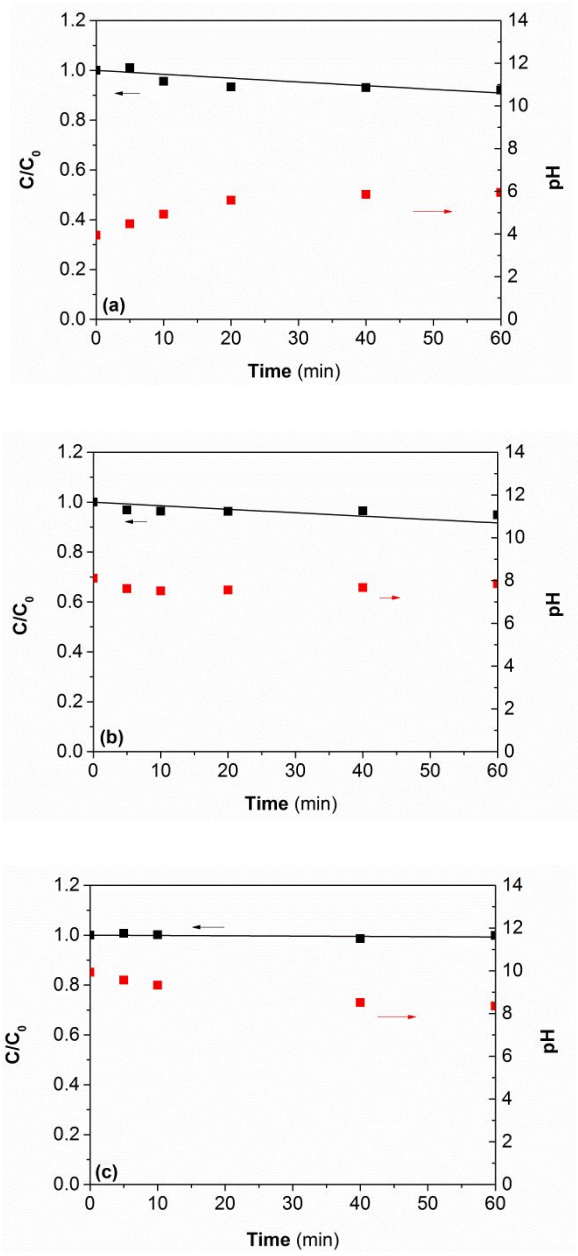

Figure S7. Changes in total As concentration (black squares) and pH (red circles) when the modified DPSC commenced with initial (a) pH 4, (b) 8 and (c) 10. Experimental conditions: the feed solution contained C_0 = 150 μg L^{-1} As(III) and 5 mM NaCl. The initial pH 4, 8 and 10 were respectively controlled by addition of HCl (<0.1 mM), 2 mM $NaHCO_3$, and 1 mM $NaHCO_3$ and 1 mM Na_2CO_3). No voltage was applied.

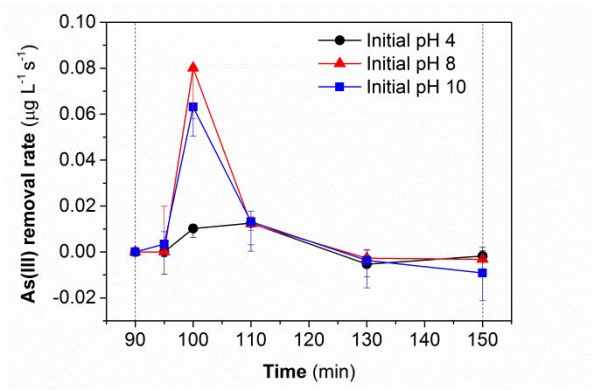

Figure S8. Changes in measured As(III) removal rate with time in the DPSC setup at varying pH conditions. Experimental conditions: the feed solution contained C_0 = 150 μg L^{-1} As(III) and 5 mM NaCl. The initial pH 4, 8 and 10 were respectively controlled by addition of HCl (<0.1 mM), 2 mM $NaHCO_3$, and 1 mM $NaHCO_3$ and 1 mM Na_2CO_3).

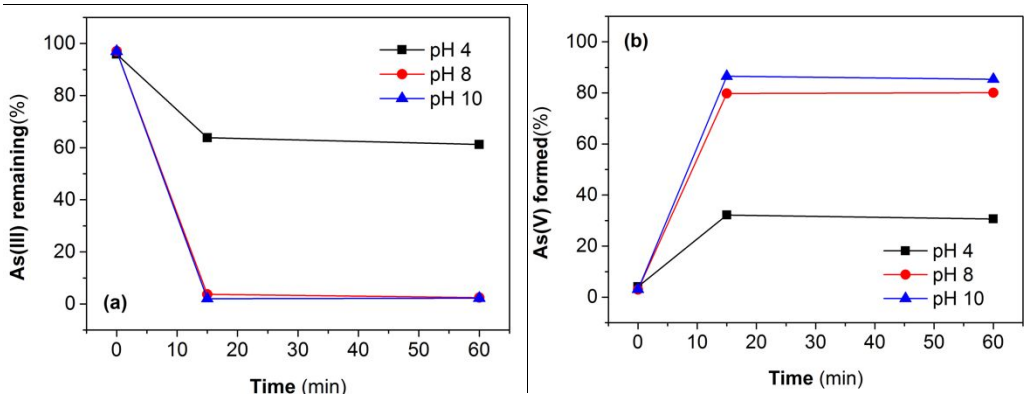

Figure S9 (a) % of As(III) remaining (b) % As(V) formed on As(III) oxidation during 60 mins when 150 μg L^{-1} As(III) is added to pH 4, 8 and 10 solution containing 160 μM H_2O_2

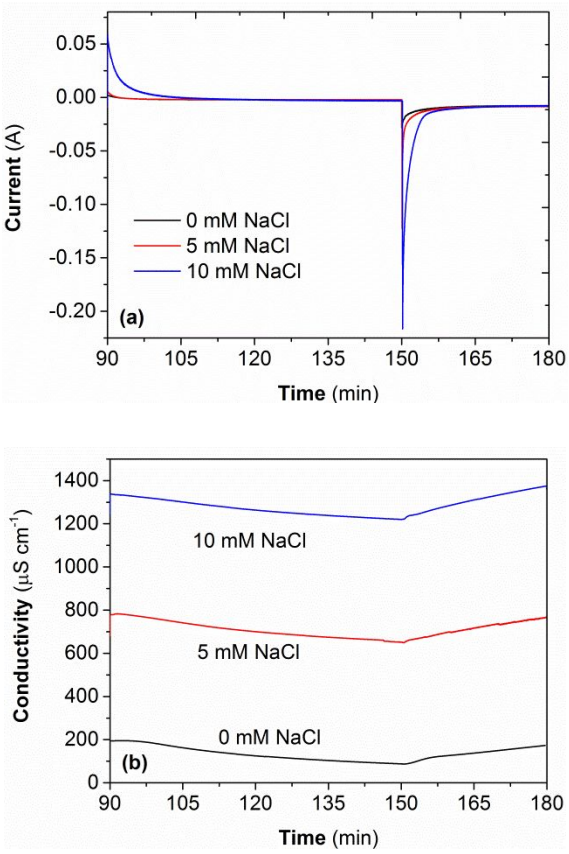

Figure S10. Changes in (a) current and (b) conductivity when the modified DPSC commenced with initial pH 8 and 0, 5 mM and 10 mM NaCl. Experimental conditions: the feed solution contained C_0 = 150 μg L^{-1} As(III). 1.2 V was applied at the first step for 60 min followed by −1.2 V for 30 min.

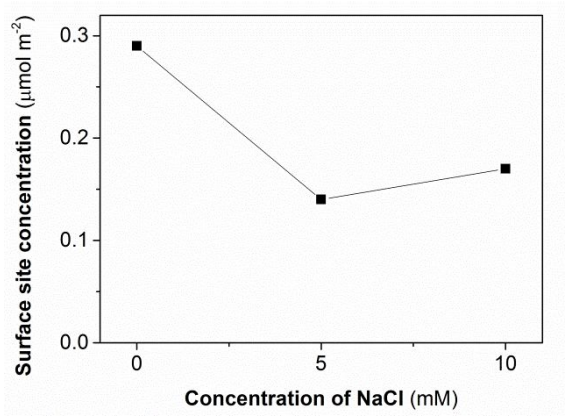

Figure S11. Surface site concentration available for As adsorption in the presence of varying NaCl concentration. (Surface site concentration: $C_S = (\Delta C \times V) / A$ where ΔC is the change in aqueous As(III) concentration; V is the volume of the batch, 60 mL; A is the surface area of the working electrode).

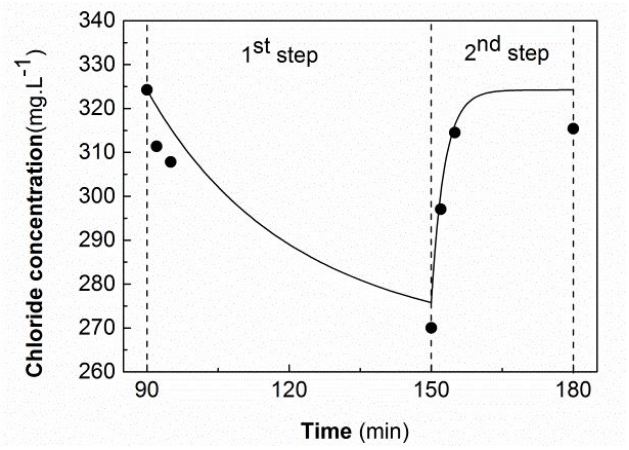

Figure S12. Change in Cl^- concentration when the modified DPSC commenced with initial 8. Experimental conditions: the feed solution contained As(V) = 150 µg L^{-1} As(III) and 5 mM NaCl. +1.2 V is applied in the 1st step followed by -1.2 V in the 2nd step.

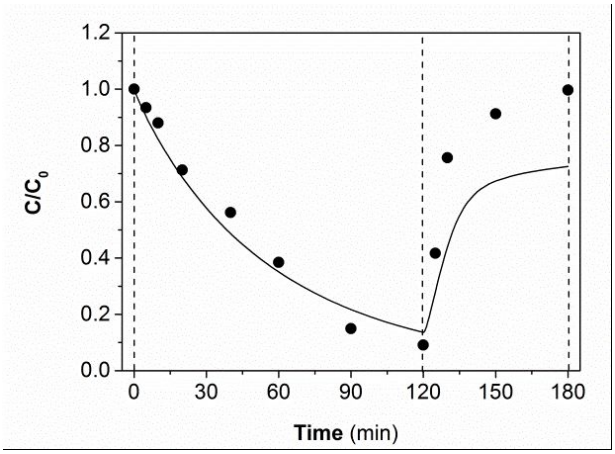

Figure S13. Changes in total arsenic concentration when 150 µg.L^{-1} As(III) is added to solution at initial pH 8 and +1.2 V is applied for 120 min followed by -1.2 V for 60 min using electrochemical cell with electrode area 10 cm × 8 cm. Symbols represent experimental data; lines represent model value.

Table S2. Parameters for the calculation of the energy cost of DPSC for removal of As(III) during 120-min adsorption in the bigger electrochemical cell

Parameters	Unit	Value
U	V	1.2
I_t	A	Figure S14
$\int_0^t I_t dt$	A.h	0.003[a]
V	m^3	0.00006
$\log\left(\frac{C_o}{C_e}\right)$		log(150/15)

[a]: the value of 0.003 represents the integrated current during step 1 over a period of 120 min.

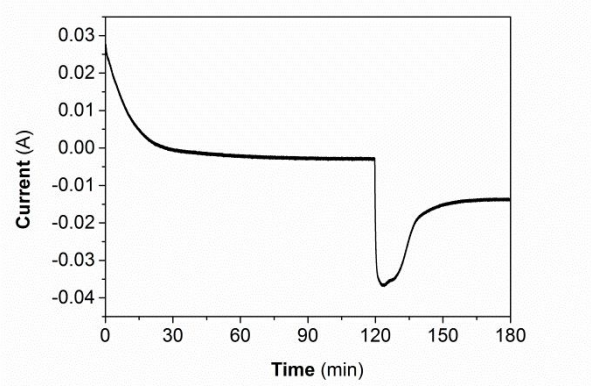

Figure S14. Change in current when the modified DPSC commenced with initial pH 8. Experimental conditions: the feed solution contained C_0 = 150 μg L^{-1} As(V) and 5 mM NaCl. The initial pH of 8 was controlled by addition of 2 mM $NaHCO_3$. 1.2 V was applied at the first step for 120 min followed by −1.2 V for 60 min in the electrochemical cell with electrode area 10 cm × 8 cm.

.

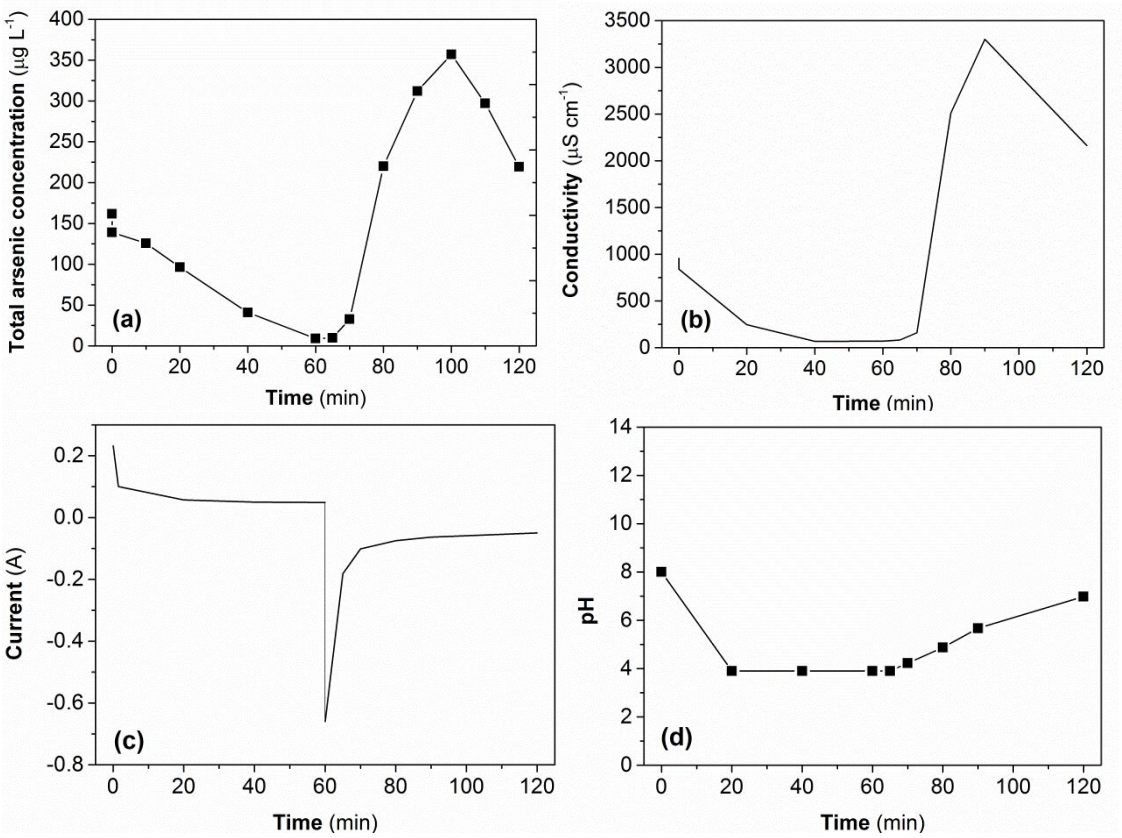

Figure S15. Changes in (a) total arsenic concentration; (b) conductivity; (c) current; (d) pH when 161 μg.L^{-1} As(III) is added to solution at initial pH 8 and +1.2 V is applied for 60 min followed by -1.2 V for 60 min using electrochemical cell with electrode area 27 cm × 17 cm shown in Figure S4 in a single-pass mode.

S3: Detailed description of the kinetic model

S3.1 Acid-base equilibrium of As(V) and As(III)

Reactions 1-8 (Table 1) represent the acid-base equilibrium reactions for the various As(III) and As(V) species. The pK_a values for these reactions were used as reported in the literature. As mentioned in the main text, we have assumed that the dominant As species in the solution and on the surface are the same and, as such, we have used the same pK_a values for adsorbed As(III) and As(V) species as that used for the dissolved species.

3.2 Physical adsorption of As(V) and As(III)

Reactions 9-12 represent the physical adsorption of As(V) and As(III) species to the working electrode. The rate constants for reactions 9 and 10 were determined based on the measured As(V) physical adsorption under varying initial pH conditions (Figure S4). The rate constants for reactions 11 and 12 were determined based on the best-fit to measured physical adsorption of As(III) under varying initial pH conditions (Figure S5). These reactions occur at the first step as well as the second step.

3.3 Electro-adsorption of Cl^-

Reaction 13 represents the electro-adsorption of chloride ions on the anode with the rate constant for this reaction determined based on the time dependence of Cl^- removal in our electrochemical cell (Figure S12).

3.4 Electro-sorption of As(III) at the anode

Reaction 14 represents the adsorption of deprotonated As(III) species when a voltage of 1.2 V is applied. Note that electro-adsorption of the neutral As(III) is expected to be negligible and hence is not included in the model.

3.5 Electro-sorption of As(V) at the anode

Reactions 15-17 represent electro-adsorption of various As(V) species. The rate constants for these reactions were determined based on the measured As(V) removal under varying initial pH conditions (Figure 2). As shown, the rate constant for electro-sorption increases with increase in charge of the As(V) species with completely deprotonated As(V) species (i.e.

AsO_4^{3-}) adsorbing at a higher rate constant compared to the protonated forms ($H_2AsO_4^-$ and $HAsO_4^-$) consistent with the observed effect of pH on As(V) electro-adsorption.

3.6 Electro-desorption of As(III)

Reaction 18 represents desorption of As(III) from the electrode when the polarity is reversed and -1.2 V voltage is applied. The rate constant for these reactions were determined based on the best fit to the measured As(III) concentration released during step 2 in Figure 4.

3.7 Electro-desorption of As(V)

Reactions 19-21 represent the desorption of As(V) when -1.2 V voltage is applied. The rate constant for these reactions were determined based on best fit to the measured As(V) concentration released during step 2 in Figures 2 and 4.

3.8 Anodic oxidation of As(III)

Reactions 22 and 23 represent the anodic oxidation of dissolved neutral and deprotonated As(III) species respectively near the electrode surface when a potential of +1.2 V is applied. Reactions 24 and 25 represents the anodic oxidation of neutral and deprotonated surface As(III) species respectively on the electrode surface when a potential of +1.2 V is applied. The rate constant for these reactions were determined based on the best fit to the measured As(III) and As(V) concentrations when As(III) is added and DPSC is commenced (Figure 4). Note that the rate constant for oxidation of the deprotonated form is higher than for neutral As(III) species which is in agreement with the reported rate constant for these species by various other oxidants such as H_2O_2. [1]

3.9 H_2O_2-mediated oxidation of As(III)

Reactions 26 and 27 represent the oxidation of As(III) by H_2O_2 that is formed on reduction of O_2 when a voltage of -1.2 V is applied. The rate constant for these reactions were determined based on the best-fit to the measured As(III) and As(V) concentrations during step 2 (Figure 4). Note that the rate constant for H_2O_2-mediated oxidation of As(III) used here is much lower than the reported rate value.[2] While the exact reason for this discrepancy is not clear, it may be due to the presence of H_2O_2 on or near the surface while As(III) is present in solution.

3.10 Non-Faradaic reactions

Reactions 28 and 29 represent the formation and consumption of protons respectively during the first and second step respectively as a result of Faradaic reactions.[2, 3] The rate constants for these reactions vary with As species present (i.e. As(III) or As(V)) and pH as well as with the potential applied and were determined based on the best-fit to measured pH values during first and second step for different initial pH values when As(V) (Figure 2c) and As(III) (Figure 3c) were added. The values of the rate constants used for various initial conditions are provided in Table S3.

Table S3 Rate constants for proton formation/consumption under different conditions.

Proton formation/consumption during As(V) removal in the first step		
pH 4	pH 8	pH 10
1×10^{-7} s^{-1}	4×10^{-8} s^{-1}	8×10^{-7} s^{-1}
0	1.5 s^{-1}	240 s^{-1}
Proton formation/consumption during As(V) removal in the second step		
pH 4	pH 8	pH 10
1×10^{-9} s^{-1}	1×10^{-20} s^{-1}	1×10^{-20} s^{-1}
4.73×10^{-3} s^{-1}	30	300 s^{-1}
Proton formation/consumption during As(III) removal in the first step		
pH 4	pH 8	pH 10
3×10^{-6} s^{-1}	9.5×10^{-8} s^{-1}	1.01×10^{-6} s^{-1}
1×10^{-2} s^{-1}	0	41 s^{-1}
Proton formation/consumption during As(III) removal in the second step		
pH 4	pH 8	pH 10
6×10^{-3} s^{-1}	800 s^{-1}	800
1×10^{-19} s^{-1}	1×10^{-19} s^{-1}	1×10^{-19} s^{-1}

3.11 Faradaic reaction resulting in H_2O_2 generation and consumption

Reactions 30-33 represent H_2O_2 formation and decay during the second step as a result of Faradaic reactions.[2, 4] The rate constants for these reactions were determined based on best-fit to the measured H_2O_2 concentration in our experimental system (Figure 5a) and were

independent of solution pH. The rate constants for the Faradaic reactions used are close to the values reported in an earlier study.[2]

References

1. E. V. i. L'udovit Molmir, Peter Lech, *Hydrometallurgy*, 1994, **35**, 1-9.
2. D. He, C. E. Wong, W. Tang, P. Kovalsky and T. D. Waite, *Environmental Science & Technology Letters*, 2016, **3**, 222-226.
3. W. Tang, D. He, C. Zhang, P. Kovalsky and T. D. Waite, *Water Res*, 2017, **120**, 229-237.
4. T. Kim, J. Yu, C. Kim and J. Yoon, *Journal of Electroanalytical Chemistry*, 2016, **776**, 101-104.